



ISSN 2053-2296

Received 24 April 2025 Accepted 23 July 2025

Edited by S. Moggach, The University of Western Australia, Australia

In memoriam Professor George M. Sheldrick (1942–2025)

Keywords: hydrazonoyl chloride; hydrogen bonding; colour polymorphism; Hirshfeld atom refinement; crystal structure.

CCDC references: 2475376; 2475377

Supporting information: this article has supporting information at journals.iucr.org/c

Concomitant colour polymorphs of (*Z*)-*N*-(4-fluorophenyl)-2-oxopropanehydrazonoyl chloride

Lisa Müller, a Richard Goddard, b Petra Frohberg and Rüdiger W. Seidela*

^aInstitut für Pharmazie, Martin-Luther-Universität Halle-Wittenberg, Wolfgang-Langenbeck-Strasse 4, 06120 Halle (Saale), Germany, and ^bMax-Planck-Institut für Kohlenforschung, Kaiser-Wilhelm-Platz 1, 45470 Mülheim an der Ruhr, Germany. *Correspondence e-mail: ruediger.seidel@pharmazie.uni-halle.de

The title compound, (Z)-N-(fluorophenyl)-2-oxopropanehydrazonoyl chloride, $C_9H_8CIFN_2O$, was found to form concomitant colour polymorphs upon recrystallization from acetone. Block-shaped pale-orange crystals of form I (space group $P2_1/n$, No. 14) and prism-shaped yellow crystals of form II (space group $P2_1/c$, No. 14) both belong to the monoclinic crystal system. $N-H\cdots O$ hydrogen bonds resulting in zigzag chains [graph-set descriptor C(6)] are the dominating intermolecular interactions in both crystal forms. The hydrogen-bonded zigzag chains so formed extend by 2_1 screw symmetry in form I and by c-glide symmetry in form II, and are arranged in layers, which are more corrugated in form II than in form I. The polymorphs are virtually indistinguishable by their calculated densities, packing indices and melting points. Form I sublimes to yield crystals of form II, whereas form II sublimes to afford crystals of the same polymorph with characteristic crystal morphology.

1. Introduction

Crystal polymorphism is the phenomenon in which a chemical compound can exist in more than one crystal form (Cruz-Cabeza et al., 2020). Thus, the atoms or molecules of the same substance can arrange into different patterns in the solid state. The different crystal forms, i.e. polymorphs, can exhibit different physical properties, such as melting point, solubility, hardness, crystal shape and optical properties, including colour. Colour polymorphism is a relatively rare phenomenon in molecular crystals, with a limited number of examples described in the literature (Nogueira et al., 2020). A unique example is 5-methyl-2-[(2-nitrophenyl)amino]thiophene-3-carbonitrile, which has up to 14 known polymorphs, the colours of which vary between red, through orange to yellow, giving rise to the acronym ROY (Weatherston et al., 2025).

In the course of our studies on heterocyclic compounds as lipoxygenase inhibitors (Frohberg *et al.*, 1995), we serendipitously discovered colour polymorphism of the precursor (*Z*)-*N*-(fluorophenyl)-2-oxopropanehydrazonoyl chloride, (1) (Scheme 1), upon recrystallization from acetone. The compound can be conveniently synthesized from 3-chloropentane-2,4-dione and 4-fluorobenzenediazonium chloride (Biere *et al.*, 1982) by employing the Japp–Klingemann reaction (Japp & Klingemann, 1888). For the synthesis and biological activity of





research papers

Table 1
Experimental details.

For both determinations: $C_0H_8CIFN_2O$, $M_r = 214.63$, Z = 4. Experiments were carried out with Mo $K\alpha$ radiation using a Bruker D8 VENTURE diffractometer. The absorption correction was Gaussian (SADABS; Bruker, 2016). All H-atom parameters were refined.

	(I)	(II)
Crystal data		
Crystal system, space group	Monoclinic, $P2_1/n$	Monoclinic, $P2_1/c$
Temperature (K)	100	101
$a, b, c (\mathring{A})$	8.3284 (10), 12.0862 (15), 9.8144 (14)	3.8945 (3), 23.3985 (15), 10.2692 (7)
β (°)	108.762 (7)	94.235 (3)
β (°) V (Å ³)	935.4 (2)	933.23 (11)
$D_x (\mathrm{Mg \ m}^{-3})$	1.524	1.528
$\mu \text{ (mm}^{-1})$	0.39	0.39
Crystal shape	Block	Prism
Colour	Pale orange	Pale yellow
Crystal size (mm)	$0.33 \times 0.23 \times 0.1$	$0.33 \times 0.13 \times 0.08$
Data collection		
T_{\min}, T_{\max}	0.919, 0.974	0.938, 0.977
No. of measured, independent and observed	260021, 2884, 2561	40492, 2872, 2641
$[I \ge 2\sigma(I)]$ reflections		
$R_{ m int}$	0.058	0.050
$(\sin \theta/\lambda)_{\max} (\mathring{A}^{-1})$	0.718	0.715
Refinement		
$R[F^2 > 2\sigma(F^2)], wR(F^2), S$	0.024, 0.075, 1.19	0.030, 0.066, 1.05
No. of reflections	2884	2872
No. of parameters	184	159
$\Delta \rho_{\text{max}}, \Delta \rho_{\text{min}} \text{ (e Å}^{-3})$	0.29, -0.21	0.24, -0.26

Computer programs: APEX5 (Bruker, 2022), SAINT (Bruker, 2019), SHELXT (Sheldrick, 2015a), olex2.refine (Bourhis et al., 2015), DIAMOND (Brandenburg, 2018), Mercury (Macrae et al., 2020) and publCIF (Westrip, 2010).

hydrazonoyl halides, we direct the interested reader to the review by Sayed *et al.* (2020). We have also investigated the solid-state structures of phenylhydrazonoyl chlorides previously (Frohberg *et al.*, 2002), but, as of now, examples characterized by X-ray crystallography remain scarce.

A search of the Cambridge Structural Database (CSD; Groom et al., 2016) for N-phenyl-2-oxopropanehydrazonoyl halides yielded the crystal structures of the unsubstituted phenyl derivative (CSD refcode XEBWIM; Abdel-Aziz et al., 2012) and the 4-methoxyphenyl (AWUXAS; Asiri et al., 2011a), 4-chlorophenyl (AWUXEW; Asiri et al., 2011b) and 4-nitrophenyl (AWUXIA; Asiri et al., 2011c) derivatives, but the title compound, (1), has not been structurally characterized by X-ray crystallography, as far as we are able to ascertain. In this article, we report the structure elucidation of two colour polymorphs of (1), which crystallized concomitantly, i.e. simultaneously, from the same solution (Bernstein et al., 1999).

2. Experimental

2.1. General

Starting materials were obtained from commercial sources and were used as received. Solvents were of reagent grade quality. NMR spectra were recorded on an Agilent Technologies 400 MHz VNMRS NMR spectrometer (abbreviations: s = singlet, d = doublet and m = multiplet). Chemical shifts are reported relative to the residual solvent signals of chloroform-d ($\delta_{\text{H}} = 7.26$ ppm and $\delta_{\text{C}} = 77.10$ ppm). Melting point determinations and sublimation experiments were performed using a

Reichert hot stage mounted on a Nikon SMZ 1500 microscope. Differential scanning calorimetry (DSC) was conducted on a Mettler Toledo Thermal Analysis System DSC 5+, using the $STAR^e$ software (Version 19.00). FT–IR spectra were recorded on a Bruker Tensor 27 spectrometer with a diamond attenuated total reflectance (ATR) unit.

2.2. Synthesis and crystallization

4-Fluoroaniline (11.1 g, 0.1 mol) was dissolved in 60 ml of hydrochloric acid (6 mol l⁻¹). After cooling to 273-278 K in an ice bath, a solution of sodium nitrite (6.9 g, 0.1 mol) in 20 ml of deionized water was added with stirring. A freshly prepared solution of 4-fluorobenzenediazonium chloride was added dropwise to a solution of 3-chloropentane-2,4-dione (13.5 g, 0.1 mol) and 40 g of anhydrous sodium acetate in 250 ml of methanol. The temperature of the reaction mixture was maintained at 278-283 K with an ice bath. After stirring for 2 h, the precipitate was separated by filtration, washed with deionized water, dried in air and recrystallized twice from acetone to yield (1) (yield: 12.02 g, 0.056 mol, 56%). ¹H NMR (402 MHz, chloroform-d): δ 8.45 (s, 1H, NH), 7.21–7.15 (m, 2H, phenyl-H), 7.07–7.00 (*m*, 2H, phenyl-H), 2.53 (*s*, 3H, CH₃) ppm. ¹³C NMR (101 MHz, chloroform-d): δ 188.2, 159.1 (d, $^{11}J_{\text{C,F}} = 242 \text{ Hz}$), 137.7 (*d*, $^{4}J_{\text{C,F}} = 3 \text{ Hz}$), 125.2, 116.3 (*d*, $^{2}J_{\text{C,F}} =$ 23 Hz), 115.8 (d, ${}^{3}J_{C,F} = 8$ Hz), 25.2 ppm.

Pale-orange crystals of form I and and pale-yellow crystals of form II suitable for single-crystal X-ray diffraction analysis were obtained when a saturated solution of (1) in acetone in a 4 ml borosilicate glass vial slowly evaporated to dryness after

standing at room temperature for several days [see Fig. S1(a) in the supporting information]. Subsequently, the two crystal forms were separated manually [Fig. S1(b)].

2.3. X-ray crystallography

The crystal structures of forms I and II were both initially refined by independent atom model (IAM) refinement using SHELXL2019 (Sheldrick, 2015b). The final structure refinement was performed with aspherical atomic form factors using NoSpherA2 (Kleemiss et al., 2021; Midgley et al., 2021) in OLEX2 (Dolomanov et al., 2009). Hirshfeld-partitioned electron density was calculated with ORCA (Version 5.0; Neese et al., 2020) using the B3LYP hybrid functional (Becke, 1993; Lee et al., 1988) and the def2-TZVPP basis set (Weigend & Ahlrichs, 2005). Positions and isotropic atomic displacement parameters were refined freely for all H atoms. For form I, atom Cl1 was refined anharmonically using a Gram Charlier expansion to fourth order implemented in OLEX2, although not strictly obeying Kuhs' rule (Kuhs, 1988), according to which an estimated resolution of $(\sin \theta/\lambda)_{\text{max}} = 0.56 \text{ Å}^{-1}$ (cf. Table 1) is required to resolve anharmonic atomic displacements. Nonetheless, the anharmonic refinement of Cl1 in form I resulted in a flat difference electron density, as compared to $\Delta \rho_{\text{max}}$, $\Delta \rho_{\text{min}} = 0.61$, -0.22 e Å⁻³ with harmonic refinement (cf. Table 1) and a decrease in $wR(F^2)$ from 0.0804 to 0.0752, despite the additional 25 parameters associated with the



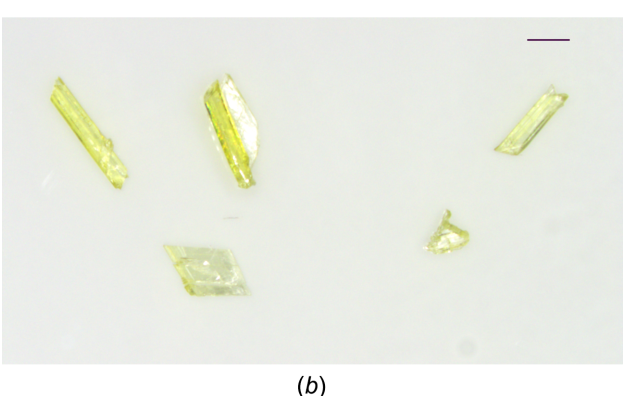


Figure 1 Microscope images of (a) crystal form I and (b) crystal form II of (1). Scale bars = 1 mm.

Table 2 Selected bond lengths and angles (\mathring{A}, \circ) for polymorphs I and II.

	Form I	Form II
C1-C2	1.5018 (11)	1.5044 (16)
C2-C3	1.4770 (12)	1.4724 (16)
C2-O1	1.2194 (10)	1.2192 (13)
C3-Cl1	1.7366 (9)	1.7342 (11)
C3-N2	1.2856 (10)	1.2908 (14)
C4-N1	1.4007 (10)	1.4055 (14)
N1-N2	1.3213 (9)	1.3117 (13)
C3-C2-C1	118.12 (7)	117.57 (10)
O1-C2-C1	122.66 (7)	122.46 (11)
Cl1-C3-C2	116.39 (6)	117.17 (8)
N2-C3-C2	121.30 (7)	119.60 (10)
N2-N1-C4	120.59 (7)	119.48 (9)
N1-N2-C3	120.28 (7)	121.70 (10)
C1-C2-C3-Cl1	178.23 (7)	-176.28 (9)
C1-C2-C3-N2	-2.23(9)	3.02 (13)
C2-C3-N2-N1	-179.70(8)	179.93 (10)
C3-N2-N1-C4	-178.69 (8)	-178.87 (11)
C5-C4-N1-N2	-5.56 (10)	-1.46 (13)

anharmonic refinement. Crystal data, data collection and structure refinement details are summarized in Table 1.

Root-mean-square (r.m.s.) deviations between the molecular structures in forms I and II were calculated with *Mercury* (Macrae *et al.*, 2020), and r.m.s. deviations of the molecules from exact point-group symmetry, as well as packing indices, were calculated with *PLATON* (Spek, 2020). Hirshfeld surface analysis was carried out with *Crystal-Explorer* (Spackman *et al.*, 2021).

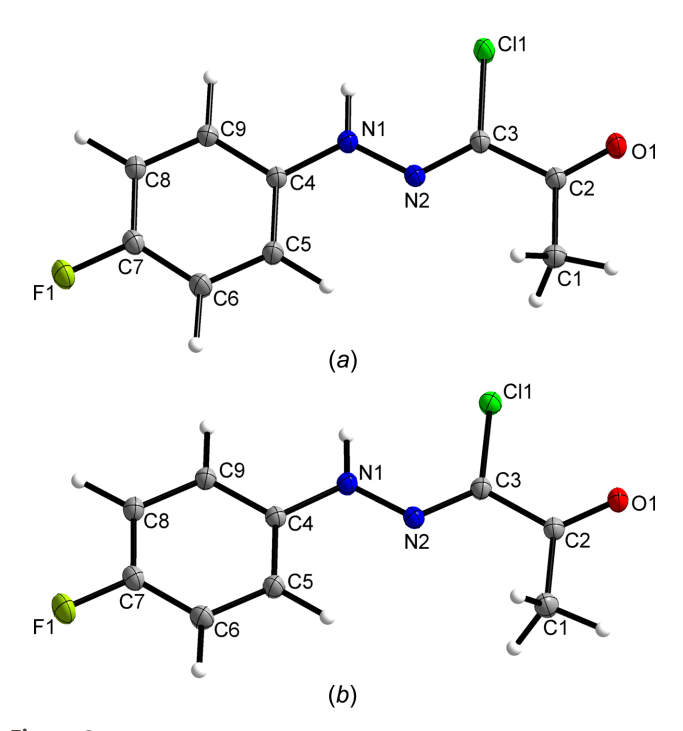


Figure 2 Displacement ellipsoid plots (50% probability) of (1) in (a) crystal form I and (b) crystal form II. H atoms are represented by small spheres of arbitrary radius.

Table 3 Hydrogen-bond geometry (Å, °) for form I.

$D-\mathrm{H}\cdots A$	D-H	$H \cdot \cdot \cdot A$	$D \cdot \cdot \cdot A$	$D-\mathrm{H}\cdots A$
N1-H1···O1i	0.973 (14)	2.013 (14)	2.9284 (10)	155.9 (11)
$C1-H1a\cdots Cl1^{ii}$	1.057 (18)	2.922 (18)	3.7917 (11)	139.9 (12)
$C1-H1c\cdots N1^{iii}$	1.042 (15)	2.805 (15)	3.5597 (12)	129.5 (10)
$C1-H1c\cdots O1^{iv}$	1.042 (15)	2.695 (15)	3.5188 (12)	135.9 (11)
$C8-H8\cdots F1^{v}$	1.071 (14)	2.653 (14)	3.6161 (11)	149.3 (10)
C9−H9···Cl1 ⁱ	1.067 (14)	2.757 (15)	3.7178 (10)	149.7 (11)
$C9-H9\cdots O1^{i}$	1.067 (14)	2.355 (14)	3.2404 (11)	139.3 (11)

Symmetry codes: (i) $-x + \frac{1}{2}$, $y - \frac{1}{2}$, $-z + \frac{1}{2}$; (ii) $-x + \frac{1}{2}$, $y + \frac{1}{2}$, $-z + \frac{1}{2}$; (iii) -x + 1, -y + 1, -z + 1; (iv) $x + \frac{1}{2}$, $-y + \frac{3}{2}$, $z + \frac{1}{2}$; (v) -x + 2, -y, -z + 1.

3. Results and discussion

The title compound, (1), was found to crystallize concomitantly in two polymorphic forms from acetone. Crystal forms I and II can be readily distinguished from one another by their colours and external shapes. Polymorph I forms block-shaped pale-orange crystals, while polymorph II forms pale-yellow prisms (Fig. 1). The crystal and molecular structures of both polymorphs were elucidated by single-crystal X-ray diffraction analysis.

Fig. 2 shows the molecular structure of (1) in both crystal forms I and II, and Table 2 compares selected bond lengths and angles. The hydrazonoyl C=N double bond was found in the Z configuration in both forms, and the C=N and C=Omoieties, as well as the C=N moiety and the 4-fluorophenyl group, adopt an anti conformation about the C2-C3 and N1—N2 formal single bonds, respectively. The same geometric arrangement of the hydrazonovl chloride group was also exclusively encountered in the crystal structures of related N-phenyl-2-oxopropanehydrazonoyl chlorides (Asiri et al., 2011a, 2011b, 2011c, 2011d; Abdel-Aziz et al., 2012; Morjan et al., 2013). In (1), the non-H-atom skeleton is essentially planar in both forms I and II, but the molecule in form II adopts a conformation closer to exact C_s point-group symmetry (r.m.s. deviation = 0.0350 Å) than in form I (r.m.s. deviation = 0.0597 Å). The larger tilt of the hydrazonovl group out of the plane of the arene group in form I compared to form II is also evident from the C5-C4-N1-N2 torsion angles (Table 2). The structure overlay plot shown in Fig. 3 illustrates the structural variation of the molecular structure in both polymorphs. By comparison, the C5-C4-N1-N2 torsion angle in the corresponding 4-methoxyphenyl derivative (AWUXAS; Asiri et al., 2011a) is even larger than in form I at 10.8° . These deviations from planarity can be attributed to packing effects.



Figure 3The molecular structures of (1) in crystal forms I (orange) and II (light green) overlaid at the C atoms of the 4-fluorophenyl group. The r.m.s. deviation of the two molecular structures from one another is 0.0925 Å.

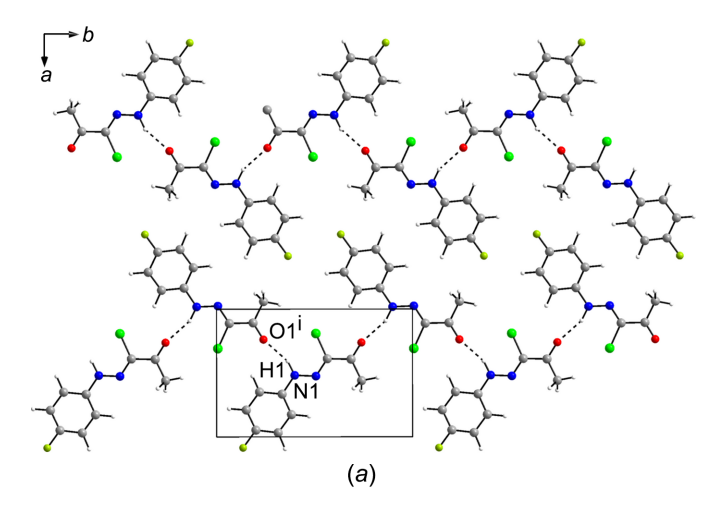
Table 4 Hydrogen-bond geometry (Å, °) for form II.

$D - H \cdot \cdot \cdot A$	D-H	$H \cdot \cdot \cdot A$	$D \cdot \cdot \cdot A$	$D - H \cdot \cdot \cdot A$
N1-H1···O1i	0.993 (16)	1.992 (16)	2.9196 (13)	154.5 (13)
$C1-H1a\cdots C11^{ii}$	1.07(2)	2.83 (2)	3.7787 (13)	148.2 (15)
$C1-H1b\cdots N2^{iii}$	1.042 (19)	2.744 (19)	3.5452 (17)	133.7 (13)
$C1-H1c\cdots F1^{iv}$	1.05(2)	2.63(2)	3.6063 (15)	153.9 (15)
$C8-H8\cdots F1^{v}$	1.079 (16)	2.576 (17)	3.6171 (14)	161.8 (12)
C9−H9···O1 ⁱ	1.066 (17)	2.364 (17)	3.2335 (14)	137.8 (13)

Symmetry codes: (i) $x+1, -y+\frac{1}{2}, z+\frac{1}{2}$; (ii) $x-1, -y+\frac{1}{2}, z-\frac{1}{2}$; (iii) x-1, y, z; (iv) -x+1, -y+1, -z+1; (v) -x+2, -y+1, -z+2.

In this context, it is worth noting that such minor conformational differences, as observed in forms I and II, do not lead to their classification as conformational polymorphs (Cruz-Cabeza & Bernstein, 2014).

Polymorphs I and II of (1) both crystallize in the monoclinic system with one molecule constituting the asymmetric unit (Z'=1). Hydrogen bonds of the N-H···O type are the prevailing intermolecular interaction in crystal forms I and II.



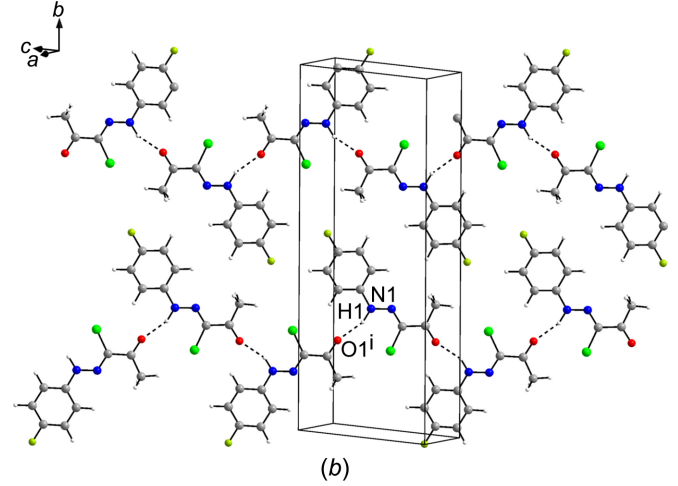


Figure 4 Hydrogen-bonded chains of (1) in (a) crystal form I (viewed along the *c*-axis direction) and (b) crystal form II [viewed towards the $(11\overline{2})$ plane], shown in relation to the monoclinic unit cells. Hydrogen bonds are shown by dashed lines. Colour scheme: C grey, H white, Cl green, F lime, N blue and O red. [Symmetry codes: (i) $-x + \frac{1}{2}$, $y - \frac{1}{2}$, $-z + \frac{1}{2}$ for part (a) and x + 1, $-y + \frac{1}{2}$, $z + \frac{1}{2}$ for part (b).]

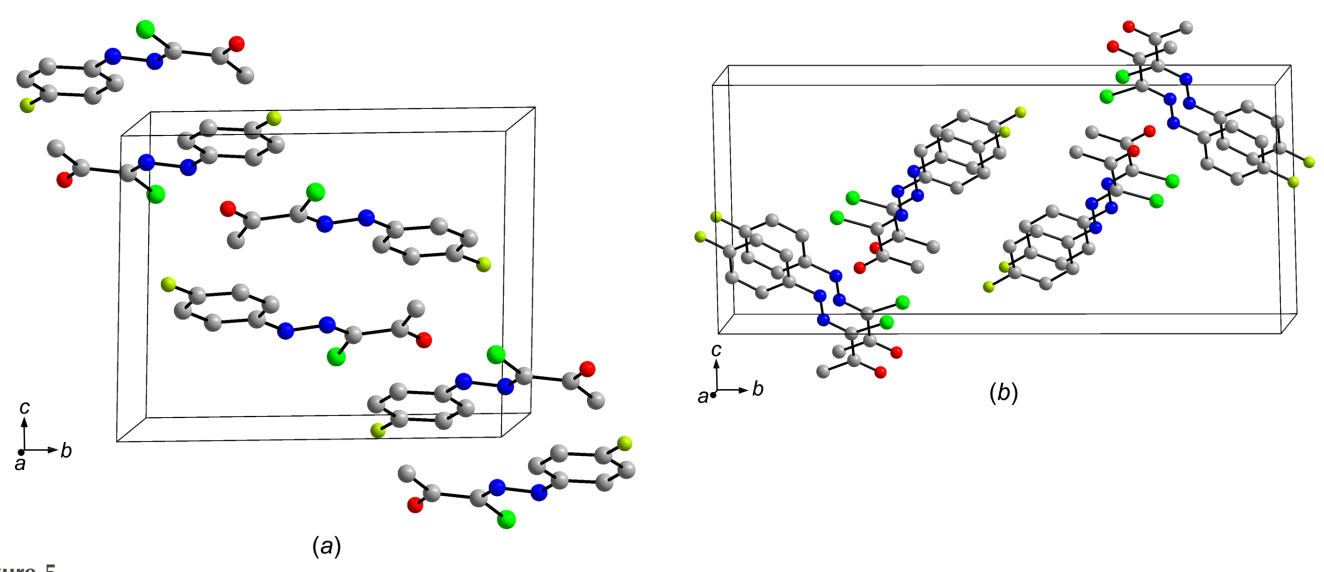


Figure 5
Packing diagrams of (1), showing the different spatial arrangement of two adjacent layers of the molecules in (a) form I and (b) form II. H atoms have been omitted for clarity.

The hydrazonoyl NH moiety forms a hydrogen bond to the carbonyl O atom of an adjacent molecule. As shown in Fig. 4, this results in zigzag chains with C(6) as the hydrogen-bond

motif descriptor (Bernstein et al., 1995) in both forms I and II. The corresponding hydrogen-bond parameters can be found in Tables 3 and 4. These fall within the expected ranges for

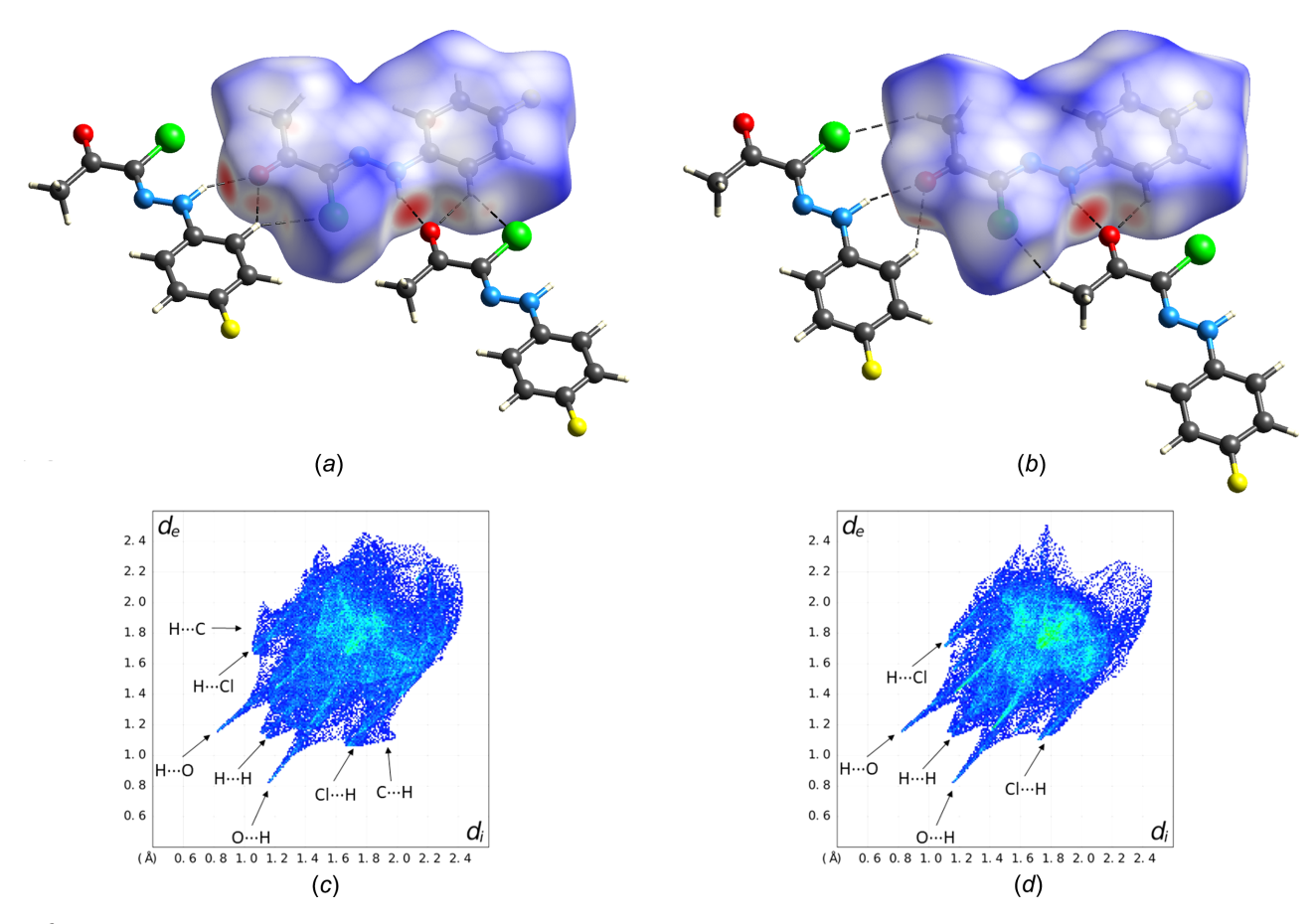
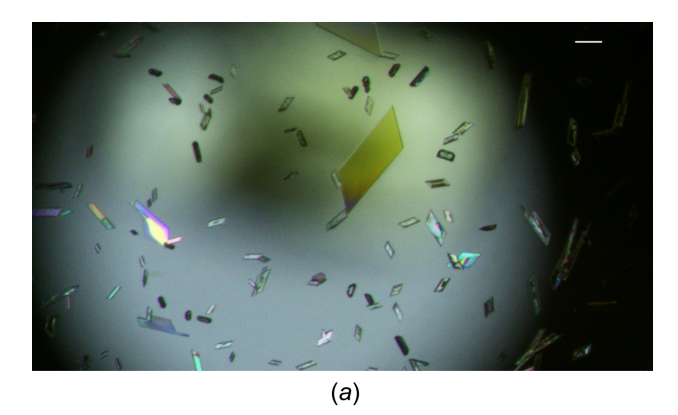
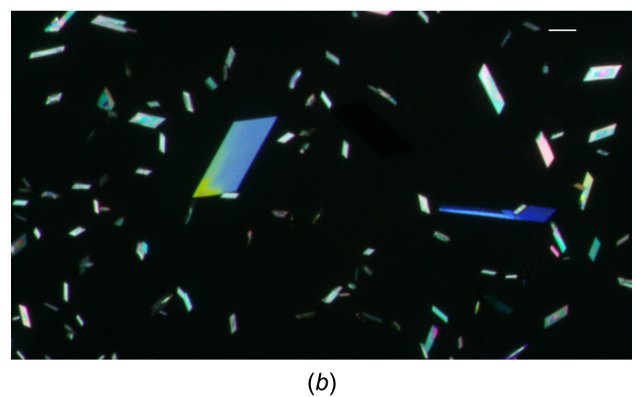


Figure 6
Hirshfeld surface mapped with d_{norm} for polymorph I (a) and II (b) of (1) and the corresponding d_e versus d_i fingerprint plots (c)/(d). d_i and d_e are the distances from a point on the Hirshfeld surface to the nearest internal and external atom, respectively. Colour scheme for the atoms: C grey, H white, Cl green, F yellow, N blue and O red.





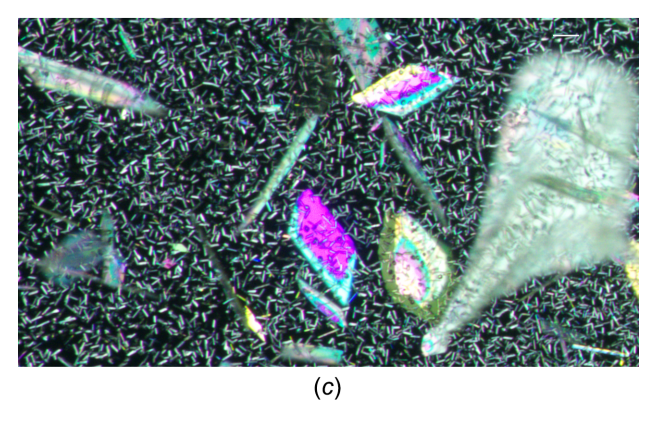


Figure 7 Crystals of (1) sublimed from (a)/(b) form I and (c) form II, showing similar morphology. Scale bars = 0.1 mm.

strong hydrogen bonds (Thakuria et al., 2017). The hydrogen-bonded chains so formed extend by 2_1 screw symmetry in form I, as also encountered in the crystal structure of the corresponding unsubstituted phenyl derivative (XEBWIM; Abdel-Aziz et al., 2012), and by glide symmetry in form II, as observed previously in the crystal structures of the 4-meth-oxyphenyl (AWUXAS; Asiri et al., 2011a), 4-chlorophenyl (AWUXEW; Asiri et al., 2011b) and 4-nitrophenyl (AWUXIA; Asiri et al., 2011c) congeners. Although both polymorphs are characterized by parallel hydrogen-bonded chains of molecules in which the 4-fluorophenyl groups dovetail into one another to create layers, it is the spatial arrangement of the layers of molecules so formed that distinguish the two polymorphs from one another. In form I, the molecules in adjacent layers parallel to $(\overline{1}03)$ form antiparallel dimers about inver-

sion centres with a distance between the mean planes through the non-H atoms of 3.27 Å [Fig. 5(a)]. In contrast, in form II, the molecules in adjacent layers parallel to $(10\overline{2})$ align in a parallel fashion with the mean planes through the molecules separated by 3.40 Å [Fig. 5(b)]. Whereas the hydrogenbonded chains are vertically offset in form I, in form II the chains are arranged above each another (Fig. S2 in the supporting information). Since the difference between the molecular conformations in both crystal forms is slight (*vide supra*), it is possible that crystal packing accounts for the different colours of polymorphs I and II (Nogueira *et al.*, 2020).

To shed light on intermolecular interactions in the crystal structures of both polymorphs by an objective identification of short contacts and in order to compare their supramolecular solid-state structures in a more quantitative manner, Hirshfeld surface analysis was performed (Spackman & Jayatilaka, 2009). Hirshfeld surface plots mapped with the normalized contact distance (d_{norm}) reveal a swapping of the shortest $H \cdot \cdot \cdot Cl$ distance from C9 $-H9 \cdot \cdot \cdot Cl1$ in polymorph I [Fig. 6(a)] to C1-H1A···Cl1 in polymorph II [Fig. 6(b)]. Red and blue coloured areas in the d_{norm} plot indicate contacts respectively shorter and longer than the van der Waals contact distance of the nearest atoms to a point on the Hirshfeld surface. The large red areas correspond to the strong N−H···O hydrogen bonds, while weak C−H···O and C−H···Cl hydrogen bonds show up as minor red areas (cf. Tables 3 and 4). The corresponding fingerprint plots are depicted in Figs. 6(c) and 6(d). As expected, both have in common the large spikes resulting from the N-H···O hydrogen bonds and the feature indicative of H···H contacts resulting from close packing. Wings that can be ascribed to C_{methyl}-H···C_{aromatic} contacts are only present for form I, whereas small spikes from C-H···Cl contacts exist for both crystal forms. The central triangular feature on the diagonal of the fingerprint plot characteristic of $C \cdot \cdot \cdot C$ contacts from $\pi - \pi$ stacking is more pronounced for form II, which is consistent with the observation that adjacent layers of molecules are offset stacked in form I.

Notably, polymorphs I and II are virtually indistinguishable by their calculated densities (Table 1), their packing indices (Kitajgorodskij, 1973), viz. 72.6% for I and 72.9% for II, and their melting points as determined by hot-stage microscopy (ca 420 K) and DSC analysis (420.7 \pm 0.3 K; see Fig. S3) (literature: 420-422 K, ethanol; Biere et al., 1982). This suggests that the energy difference between the two polymorphs is small, which possibly accounts for their concomitant crystallization from acetone. Samples of both forms I and II began to sublime on the hot stage between about 373 K and the melting points. The crystals deposited by sublimation exhibited similar morphology and unit-cell parameters corresponding to those of form II (Figs. 7 and S4). As expected, both polymorphs are also nearly indistinguishable with respect to their IR spectra in the region 4000–400 cm⁻¹ (see Fig. S5). The bands that can be assigned to the N-H and C=O stretching vibrations were observed at 3231 (form I) and 3234 (form II), and 1680 (form I) and 1678 cm^{-1} (form II), respectively. Since mid-IR spectroscopy mainly probes vibrations associated with functional groups, it cannot readily discriminate between polymorphs with similar molecular structures and similar hydrogen-bonding patterns as observed here (Suresh *et al.*, 2019).

4. Conclusions

We have discovered concomitant colour polymorphism of compound (I) by serendipity. X-ray crystallography revealed that the two colour polymorphs have in common a nearly planar molecular conformation of the non-H-atom skeleton and the intermolecular one-periodic hydrogen-bonding pattern. In contrast, the spatial arrangement of the hydrogenbonded chains is distinctly different in both polymorphs, albeit with virtually similar packing efficiency, as revealed by the calculated densities and packing indices. Polymorph I is characterized by offset stacking of the molecules with an antiparallel alignment between the closest molecules, whereas the molecules in polymorph II stack in a parallel fashion. The results suggest that the colour difference between the two polymorphs may result from the different crystal packing rather than different molecular conformations in the solid state.

Acknowledgements

We would like to thank Professor Christian W. Lehmann for providing access to the X-ray diffraction facility, and Heike Schucht and Lucas Schulte-Zweckel for technical assistance with the X-ray intensity data collections. Peter Bamfaste (Mettler–Toledo International Inc., Giessen, Germany) is gratefully acknowledged for performing the DSC analyses. Open access funding enabled and organized by Projekt DEAL.

References

- Abdel-Aziz, H. A., Chia, T. S. & Fun, H.-K. (2012). *Acta Cryst.* E**68**, o2263.
- Asiri, A. M., Al-Youbi, A. O., Zayed, M. E. M. & Ng, S. W. (2011a). Acta Cryst. E67, o1961.
- Asiri, A. M., Al-Youbi, A. O., Zayed, M. E. M. & Ng, S. W. (2011b).
 Acta Cryst. E67, o1962.
- Asiri, A. M., Al-Youbi, A. O., Zayed, M. E. M. & Ng, S. W. (2011c). Acta Cryst. E67, o1963.
- Asiri, A. M., Al-Youbi, A. O., Zayed, M. E. M. & Ng, S. W. (2011d). Acta Cryst. E67, o1964.
- Becke, A. D. (1993). J. Chem. Phys. 98, 5648-5652.
- Bernstein, J., Davey, R. J. & Henck, J.-O. (1999). *Angew. Chem. Intl Ed.* **38**, 3440–3461.
- Bernstein, J., Davis, R. E., Shimoni, L. & Chang, N.-L. (1995). *Angew. Chem. Int. Ed. Engl.* **34**, 1555–1573.
- Biere, H., Schröder, E., Ahrens, H., Kapp, J.-F. & Böttcher, I. (1982). *Eur. J. Med. Chem.* **17**, 27–34.

- Bourhis, L. J., Dolomanov, O. V., Gildea, R. J., Howard, J. A. K. & Puschmann, H. (2015). *Acta Cryst.* A71, 59–75.
- Brandenburg, K. (2018). *DIAMOND*. Crystal Impact GbR, Bonn, Germany.
- Bruker (2016). SADABS. Bruker AXS Inc., Madison, Wisconsin, USA.
- Bruker (2019). SAINT. Bruker AXS Inc., Madison, Wisconsin, USA.
- Bruker (2022). APEX5. Bruker AXS Inc., Madison, Wisconsin, USA. Cruz-Cabeza, A. & Bernstein, J. (2014). Chem. Rev. 114, 2170–2191.
- Cruz-Cabeza, A., Feeder, N. & Davey, R. J. (2020). *Commun. Chem.* **3.** 142.
- Dolomanov, O. V., Bourhis, L. J., Gildea, R. J., Howard, J. A. K. & Puschmann, H. (2009). J. Appl. Cryst. 42, 339–341.
- Frohberg, P., Drutkowski, G. & Wagner, C. (2002). *Eur. J. Org. Chem.* **2002**, 1654–1663.
- Frohberg, P., Kupfer, C., Stenger, P., Baumeister, U. & Nuhn, P. (1995). Arch. Pharm. 328, 505-516.
- Groom, C. R., Bruno, I. J., Lightfoot, M. P. & Ward, S. C. (2016). Acta Cryst. B72, 171–179.
- Japp, F. R. & Klingemann, F. (1888). Justus Liebigs Ann. Chem. 247, 190–225.
- Kitajgorodskij, A. I. (1973). In *Molecular crystals and molecules*. London: Academic Press.
- Kleemiss, F., Dolomanov, O. V., Bodensteiner, M., Peyerimhoff, N., Midgley, M., Bourhis, L. J., Genoni, A., Malaspina, L. A., Jayatilaka, D., Spencer, J. L., White, F., Grundkötter-Stock, B., Steinhauer, S., Lentz, D., Puschmann, H. & Grabowsky, S. (2021). *Chem. Sci.* 12, 1675–1692.
- Kuhs, W. F. (1988). Aust. J. Phys. 41, 369-382.
- Lee, C., Yang, W. & Parr, R. G. (1988). Phys. Rev. B 37, 785-789.
- Macrae, C. F., Sovago, I., Cottrell, S. J., Galek, P. T. A., McCabe, P., Pidcock, E., Platings, M., Shields, G. P., Stevens, J. S., Towler, M. & Wood, P. A. (2020). *J. Appl. Cryst.* **53**, 226–235.
- Midgley, L., Bourhis, L. J., Dolomanov, O. V., Grabowsky, S., Kleemiss, F., Puschmann, H. & Peyerimhoff, N. (2021). *Acta Cryst.* A77, 519–533.
- Morjan, R. Y., Abu Thaher, B. A., Schollmeyer, D., Awadallah, A. M. & Gardiner, J. M. (2013). *Acta Cryst.* E69, 072.
- Neese, F., Wennmohs, F., Becker, U. & Riplinger, C. (2020). *J. Chem. Phys.* **152**, 224108.
- Nogueira, B. A., Castiglioni, C. & Fausto, R. (2020). *Commun. Chem.* **3**, 34.
- Sayed, A. R., Ali, S. H., Gomha, S. M. & Al-Faiyz, Y. S. (2020). Synth. Commun. 50, 3175–3203.
- Sheldrick, G. M. (2015a). Acta Cryst. A71, 3-8.
- Sheldrick, G. M. (2015b). Acta Cryst. C71, 3-8.
- Spackman, M. A. & Jayatilaka, D. (2009). CrystEngComm 11, 19–32.
 Spackman, P. R., Turner, M. J., McKinnon, J. J., Wolff, S. K., Grimwood, D. J., Jayatilaka, D. & Spackman, M. A. (2021). J. Appl. Cryst. 54, 1006–1011.
- Spek, A. L. (2020). Acta Cryst. E76, 1-11.
- Suresh, K., Ashe, J. S. & Matzger, A. J. (2019). *J. Pharm. Sci.* **108**, 1915–1920.
- Thakuria, R., Sarma, B. & Nangia, A. (2017). Hydrogen bonding in molecular crystals, in Comprehensive supramolecular chemistry II, Vol. 7, edited by J. L. Atwood, pp. 25–48. Oxford: Elsevier.
- Weatherston, J., Probert, M. R. & Hall, M. J. (2025). *J. Am. Chem. Soc.* **147**, 11949–11954.
- Weigend, F. & Ahlrichs, R. (2005). *Phys. Chem. Chem. Phys.* **7**, 3297–3305.
- Westrip, S. P. (2010). J. Appl. Cryst. 43, 920-925.

Acta Cryst. (2025). C81, 481-487 [https://doi.org/10.1107/S2053229625006618]

Concomitant colour polymorphs of (*Z*)-*N*-(4-fluorophenyl)-2-oxopropane-hydrazonoyl chloride

Lisa Müller, Richard Goddard, Petra Frohberg and Rüdiger W. Seidel

Computing details

(Z)-N-(4-Fluorophenyl)-2-oxopropanehydrazonoyl chloride (I)

Crystal data

 $C_9H_8C1FN_2O$

 $M_r = 214.63$

Monoclinic, $P2_1/n$

a = 8.3284 (10) Å

b = 12.0862 (15) Å

c = 9.8144 (14) Å

 $\beta = 108.762 (7)^{\circ}$

 $V = 935.4 (2) \text{ Å}^3$

Z = 4

Data collection

Bruker D8 VENTURE

diffractometer

Radiation source: microfocus X-ray tube Montel multilayer optics monochromator

Detector resolution: 7.391 pixels mm⁻¹

 φ and ω scans

Absorption correction: gaussian

(SADABS; Bruker, 2016)

 $T_{\min} = 0.919, T_{\max} = 0.974$

Refinement

Refinement on F^2

Least-squares matrix: full

 $R[F^2 > 2\sigma(F^2)] = 0.024$

 $wR(F^2) = 0.075$

S = 1.19

2884 reflections

184 parameters

0 restraints

0 constraints

Primary atom site location: dual

F(000) = 440.892

 $D_x = 1.524 \text{ Mg m}^{-3}$

Mo $K\alpha$ radiation, $\lambda = 0.71073 \text{ Å}$

Cell parameters from 9127 reflections

 $\theta = 2.8 - 30.5^{\circ}$

 $\mu = 0.39 \text{ mm}^{-1}$

T = 100 K

Block, pale orange

 $0.33 \times 0.23 \times 0.1 \text{ mm}$

260021 measured reflections

2884 independent reflections 2561 reflections with $I \ge 2\sigma(I)$

 $R_{\rm int} = 0.058$

 $\theta_{\rm max} = 30.7^{\circ}, \ \theta_{\rm min} = 2.8^{\circ}$

 $h = -11 \rightarrow 11$

 $k = -17 \longrightarrow 17$

 $l = -14 \rightarrow 14$

Secondary atom site location: difference Fourier

mar

Hydrogen site location: difference Fourier map

All H-atom parameters refined

 $w = 1/[\sigma^2(F_0^2) + (0.0364P)^2 + 0.1803P]$

where $P = (F_0^2 + 2F_c^2)/3$

 $(\Delta/\sigma)_{\text{max}} = 0.001$

 $\Delta \rho_{\text{max}} = 0.29 \text{ e Å}^{-3}$

 $\Delta \rho_{\min} = -0.21 \text{ e Å}^{-3}$

Special details

Experimental. Crystal mounted on a MiTeGen loop using Perfluoropolyether Fomblin YR-1800

Refinement. Refinement using NoSpherA2, an implementation of NOn-SPHERical Atom-form-factors in Olex2. Please cite: F. Kleemiss *et al.* Chem. Sci. DOI 10.1039/D0SC05526C - 2021 NoSpherA2 implementation of HAR makes use of tailor-made aspherical atomic form factors calculated on-the-fly from a Hirshfeld-partitioned electron density (ED) - not from spherical-atom form factors.

The ED is calculated from a gaussian basis set single determinant SCF wavefunction - either Hartree-Fock or DFT using selected funtionals - for a fragment of the crystal. This fragment can be embedded in an electrostatic crystal field by employing cluster charges or modelled using implicit solvation models, depending on the software used. The following options were used: SOFTWARE: ORCA 5.0 PARTITIONING: NoSpherA2 INT ACCURACY: Normal METHOD: B3LYP BASIS SET: def2-TZVPP CHARGE: 0 MULTIPLICITY: 1 DATE: 2025-01-22 17-57-39

Fractional atomic coordinates and isotropic or equivalent isotropic displacement parameters (\mathring{A}^2)

	x	у	Z	$U_{ m iso}$ */ $U_{ m eq}$
C1	0.55964 (11)	0.74002 (7)	0.38904 (10)	0.02145 (17)
H1a	0.536(2)	0.8219 (15)	0.4151 (17)	0.063 (4)*
H1b	0.637(2)	0.7388 (13)	0.3235 (17)	0.060 (4)*
H1c	0.6204 (19)	0.6998 (13)	0.4858 (16)	0.054 (4)*
C2	0.39247 (10)	0.68649 (7)	0.31138 (9)	0.01852 (16)
C3	0.38845 (10)	0.56517 (7)	0.29251 (9)	0.01885 (16)
C4	0.66536 (10)	0.33425 (7)	0.36891 (9)	0.01747 (15)
C5	0.82533 (10)	0.38172 (7)	0.42928 (10)	0.02267 (17)
H5	0.8385 (18)	0.4717 (12)	0.4373 (15)	0.044 (4)*
C6	0.96718 (11)	0.31391 (8)	0.48054 (10)	0.02444 (18)
Н6	1.0941 (18)	0.3489 (11)	0.5254 (14)	0.038 (3)*
C7	0.94670 (10)	0.20029 (7)	0.47048 (9)	0.02035 (16)
C8	0.78956 (10)	0.15145 (7)	0.41019 (9)	0.02034 (16)
Н8	0.7792 (17)	0.0632 (11)	0.4021 (13)	0.037 (3)*
C9	0.64802 (10)	0.21914 (7)	0.35871 (9)	0.01934 (16)
H9	0.5247 (18)	0.1836 (12)	0.3154 (15)	0.045 (4)*
Cl1	0.19129 (7)	0.50672 (4)	0.20658 (7)	0.0281 (2)
F1	1.08516 (7)	0.13484 (5)	0.51914 (6)	0.02700 (14)
N1	0.51812 (9)	0.39852 (6)	0.31827 (8)	0.01963 (15)
H1	0.4083 (18)	0.3633 (11)	0.2753 (15)	0.036 (3)*
N2	0.52454 (9)	0.50690 (6)	0.33685 (8)	0.01801 (14)
O1	0.26156 (8)	0.73918 (5)	0.26285 (7)	0.02385 (15)

Atomic displacement parameters (\mathring{A}^2)

	U^{11}	U^{22}	U^{33}	U^{12}	U^{13}	U^{23}
C1	0.0162 (4)	0.0176 (4)	0.0283 (4)	-0.0008 (3)	0.0039 (3)	-0.0012 (3)
C2	0.0142(3)	0.0142(3)	0.0250(4)	0.0011 (3)	0.0034(3)	0.0000(3)
C3	0.0145 (3)	0.0135(3)	0.0265 (4)	0.0013 (3)	0.0038(3)	-0.0005(3)
C4	0.0138(3)	0.0132(3)	0.0236(3)	0.0008(3)	0.0034(3)	0.0006(3)
C5	0.0149(3)	0.0138 (4)	0.0355 (4)	0.0004(3)	0.0029(3)	-0.0010(3)
C6	0.0140(3)	0.0177 (4)	0.0367 (5)	0.0010(3)	0.0013(3)	-0.0018(3)
C7	0.0155(3)	0.0174 (4)	0.0259 (4)	0.0031 (3)	0.0034(3)	0.0010(3)
C8	0.0170(3)	0.0144 (4)	0.0285 (4)	0.0020(3)	0.0058(3)	0.0012(3)

Acta Cryst. (2025). C81, 481-487 sup-2

C9	0.0147 (3)	0.0140(3)	0.0280 (4)	0.0002(3)	0.0051(3)	0.0004(3)
Cl1	0.0138 (4)	0.0147 (4)	0.0486 (5)	0.0007(2)	0.0003(3)	-0.0046(2)
F1	0.0183 (2)	0.0222(3)	0.0362(3)	0.00657 (19)	0.0027(2)	0.0015 (2)
N1	0.0138 (3)	0.0139(3)	0.0285(3)	0.0010(2)	0.0031 (3)	0.0001 (2)
N2	0.0135 (3)	0.0145 (3)	0.0244(3)	0.0011(2)	0.0039(2)	0.0005 (2)
O1	0.0156 (3)	0.0151 (3)	0.0361 (3)	0.0024 (2)	0.0016(2)	-0.0008 (2)

Geometric parameters (Å, °)

C1—H1a	1.057 (18)	C5—H5	1.093 (15)
C1—H1b	1.047 (16)	C5—C6	1.3923 (12)
C1—H1c	1.042 (15)	C6—H6	1.091 (14)
C1—C2	1.5018 (11)	C6—C7	1.3834 (12)
C2—C3	1.4770 (12)	C7—C8	1.3832 (12)
C2—O1	1.2194 (10)	C7—F1	1.3525 (9)
C3—C11	1.7366 (9)	C8—H8	1.071 (14)
C3—N2	1.2856 (10)	C8—C9	1.3896 (11)
C4—C5	1.3955 (11)	С9—Н9	1.067 (14)
C4—C9	1.3990 (11)	N1—H1	0.973 (14)
C4—N1	1.4007 (10)	N1—N2	1.3213 (9)
H1b—C1—H1a	111.3 (12)	C6—C5—H5	120.4 (7)
H1c-C1-H1a	106.9 (12)	H6—C6—C5	121.1 (7)
H1c-C1-H1b	109.8 (11)	C7—C6—C5	119.19 (8)
C2—C1—H1a	108.0 (9)	C7—C6—H6	119.7 (7)
C2—C1—H1b	109.6 (9)	C8—C7—C6	122.15 (8)
C2—C1—H1c	111.2 (8)	F1—C7—C6	118.94 (7)
C3—C2—C1	118.12 (7)	F1—C7—C8	118.90 (7)
O1—C2—C1	122.66 (7)	H8—C8—C7	120.0 (7)
O1—C2—C3	119.22 (7)	C9—C8—C7	118.65 (8)
C11—C3—C2	116.39 (6)	C9—C8—H8	121.4 (7)
N2—C3—C2	121.30 (7)	C8—C9—C4	120.23 (7)
N2—C3—C11	122.31 (7)	H9—C9—C4	119.5 (8)
C9—C4—C5	120.11 (7)	H9—C9—C8	120.2 (8)
N1—C4—C5	122.00 (7)	H1—N1—C4	120.3 (8)
N1—C4—C9	117.88 (7)	N2—N1—C4	120.59 (7)
H5—C5—C4	120.0 (7)	N2—N1—H1	119.0 (8)
C6—C5—C4	119.65 (8)	N1—N2—C3	120.28 (7)
C1—C2—C3—C11	178.23 (7)	C4—C9—C8—C7	-0.36 (10)
C1—C2—C3—N2	-2.23 (9)	C5—C6—C7—C8	0.40 (11)
C2—C3—N2—N1	-179.70(8)	C5—C6—C7—F1	179.35 (8)
C3—N2—N1—C4	-178.69 (8)	C6—C7—C8—C9	-0.24 (11)
C4—C5—C6—C7	0.05 (11)		

Acta Cryst. (2025). C81, 481-487 sup-3

Hydrogen-bond geometry (Å, °)

D— H ··· A	D—H	$H\cdots A$	D··· A	D— H ··· A
N1—H1···O1 ⁱ	0.973 (14)	2.013 (14)	2.9284 (10)	155.9 (11)
C1—H1a···Cl1 ⁱⁱ	1.057 (18)	2.922 (18)	3.7917 (11)	139.9 (12)
C1—H1 <i>c</i> ···N1 ⁱⁱⁱ	1.042 (15)	2.805 (15)	3.5597 (12)	129.5 (10)
C1—H1 <i>c</i> ···O1 ^{iv}	1.042 (15)	2.695 (15)	3.5188 (12)	135.9 (11)
C8—H8···F1 ^v	1.071 (14)	2.653 (14)	3.6161 (11)	149.3 (10)
C9—H9···Cl1 ⁱ	1.067 (14)	2.757 (15)	3.7178 (10)	149.7 (11)
C9—H9···O1 ⁱ	1.067 (14)	2.355 (14)	3.2404 (11)	139.3 (11)

Symmetry codes: (i) -x+1/2, y-1/2, -z+1/2; (ii) -x+1/2, y+1/2, -z+1/2; (iii) -x+1, -y+1, -z+1; (iv) x+1/2, -y+3/2, z+1/2; (v) -x+2, -y, -z+1.

(Z)-N-(4-Fluorophenyl)-2-oxopropanehydrazonoyl chloride (II)

Crystal data

 $C_9H_8CIFN_2O$ $M_r = 214.63$ Monoclinic, $P2_1/c$ a = 3.8945 (3) Å b = 23.3985 (15) Å c = 10.2692 (7) Å $\beta = 94.235$ (3)° V = 933.23 (11) Å³ Z = 4

Data collection

Bruker D8 VENTURE

diffractometer Radiation source: microfocus X-ray tube Montel multilayer optics monochromator Detector resolution: 7.391 pixels mm⁻¹ φ and ω scans

Absorption correction: gaussian (SADABS; Bruker, 2016) $T_{min} = 0.938$, $T_{max} = 0.977$

Refinement

Refinement on F^2

Least-squares matrix: full $R[F^2 > 2\sigma(F^2)] = 0.030$ $wR(F^2) = 0.066$ S = 1.05 2872 reflections 159 parameters 0 restraints 0 constraints

Primary atom site location: dual

F(000) = 440.892 $D_x = 1.528 \text{ Mg m}^{-3}$ Mo $K\alpha$ radiation, $\lambda = 0.71073 \text{ Å}$ Cell parameters from 9923 reflections $\theta = 2.6-30.4^{\circ}$ $\mu = 0.39 \text{ mm}^{-1}$ T = 101 KPrism, pale yellow

40492 measured reflections 2872 independent reflections 2641 reflections with $I \ge 2\sigma(I)$ $R_{\text{int}} = 0.050$ $\theta_{\text{max}} = 30.6^{\circ}, \, \theta_{\text{min}} = 2.2^{\circ}$ $h = -5 \rightarrow 5$ $k = -33 \rightarrow 33$ $l = -14 \rightarrow 12$

 $0.33 \times 0.13 \times 0.08 \text{ mm}$

Secondary atom site location: difference Fourier map

Hydrogen site location: difference Fourier map All H-atom parameters refined

w = $1/[\sigma^2(F_o^2) + (0.P)^2 + 0.7054P]$ where $P = (F_o^2 + 2F_c^2)/3$

 $(\Delta/\sigma)_{\rm max} = 0.0001$ $\Delta\rho_{\rm max} = 0.24 \text{ e Å}^{-3}$ $\Delta\rho_{\rm min} = -0.26 \text{ e Å}^{-3}$

Special details

Experimental. Crystal mounted on a MiTeGen loop using perfluoropolyether Fomblin YR-1800

Refinement. Refinement using NoSpherA2, an implementation of NOn-SPHERical Atom-form-factors in Olex2. Please cite: F. Kleemiss *et al.* Chem. Sci. DOI 10.1039/D0SC05526C - 2021 NoSpherA2 implementation of HAR makes use of tailor-made aspherical atomic form factors calculated on-the-fly from a Hirshfeld-partitioned electron density (ED) - not from spherical-atom form factors.

The ED is calculated from a gaussian basis set single determinant SCF wavefunction - either Hartree-Fock or DFT using selected funtionals - for a fragment of the crystal. This fragment can be embedded in an electrostatic crystal field by employing cluster charges or modelled using implicit solvation models, depending on the software used. The following options were used: SOFTWARE: ORCA 5.0 PARTITIONING: NoSpherA2 INT ACCURACY: Normal METHOD: B3LYP BASIS SET: def2-TZVPP CHARGE: 0 MULTIPLICITY: 1 DATE: 2025-01-29 23-46-08

Fractional atomic coordinates and isotropic or equivalent isotropic displacement parameters (\mathring{A}^2)

	x	y	Z	$U_{ m iso}$ */ $U_{ m eq}$
C11	0.23372 (8)	0.222533 (11)	0.48534(3)	0.01943 (7)
F1	0.6799(2)	0.53726 (3)	0.86529 (8)	0.02930 (18)
N1	0.3728 (3)	0.33596 (4)	0.60290 (9)	0.01736 (19)
H1	0.463 (4)	0.2996 (7)	0.6419 (16)	0.028 (4)*
N2	0.1836 (2)	0.33627 (4)	0.49179 (9)	0.01646 (18)
O1	-0.2019(2)	0.24825 (4)	0.24948 (8)	0.02297 (19)
C1	-0.2098(3)	0.35043 (5)	0.25284 (13)	0.0220 (2)
H1a	-0.359(6)	0.3468 (9)	0.162(2)	0.064 (6)*
H1b	-0.359(5)	0.3717 (8)	0.3176 (19)	0.053 (5)*
H1c	0.005 (5)	0.3762 (8)	0.2383 (19)	0.058 (5)*
C2	-0.1120(3)	0.29225 (5)	0.30576 (11)	0.0171 (2)
C3	0.1012(3)	0.28961 (4)	0.43012 (11)	0.0164 (2)
C4	0.4502(3)	0.38788 (5)	0.66736 (11)	0.0157 (2)
C5	0.3362(3)	0.43999 (5)	0.61407 (11)	0.0191 (2)
H5	0.183 (4)	0.4420 (7)	0.5221 (16)	0.033 (4)*
C6	0.4145 (3)	0.49046 (5)	0.68154 (12)	0.0210 (2)
H6	0.326 (4)	0.5309 (7)	0.6438 (16)	0.037 (4)*
C7	0.6035 (3)	0.48790 (5)	0.80058 (12)	0.0202 (2)
C8	0.7201 (3)	0.43675 (5)	0.85509 (11)	0.0196 (2)
H8	0.873 (4)	0.4361 (7)	0.9471 (16)	0.033 (4)*
C9	0.6429 (3)	0.38624 (5)	0.78741 (11)	0.0181 (2)
Н9	0.740 (4)	0.3465 (7)	0.8248 (17)	0.043 (5)*

Atomic displacement parameters (\mathring{A}^2)

	U^{11}	U^{22}	U^{33}	U^{12}	U^{13}	U^{23}
Cl1	0.02570 (14)	0.01425 (12)	0.01766 (12)	0.00125 (10)	-0.00291 (10)	-0.00039 (9)
F1	0.0417 (5)	0.0177(3)	0.0275 (4)	-0.0034(3)	-0.0042(3)	-0.0068(3)
N1	0.0227 (5)	0.0134 (4)	0.0154 (4)	0.0006(3)	-0.0028(4)	-0.0010(3)
N2	0.0200 (5)	0.0131 (4)	0.0159 (4)	-0.0005(3)	-0.0015(3)	-0.0009(3)
O1	0.0330 (5)	0.0166 (4)	0.0180(4)	-0.0042(3)	-0.0067(3)	-0.0009(3)
C1	0.0253 (6)	0.0172 (5)	0.0224 (6)	-0.0005(4)	-0.0055(5)	0.0014 (4)
C2	0.0191 (5)	0.0154 (5)	0.0163 (5)	-0.0018 (4)	-0.0024(4)	-0.0005(4)
C3	0.0202 (5)	0.0142 (5)	0.0144 (5)	0.0003 (4)	-0.0017(4)	-0.0008(4)

Acta Cryst. (2025). C81, 481-487 sup-5

C4	0.0188 (5)	0.0135 (5)	0.0144 (5)	-0.0003 (4)	-0.0009(4)	-0.0006(4)	
C5	0.0249 (6)	0.0140 (5)	0.0174 (5)	0.0002 (4)	-0.0040(4)	-0.0001(4)	
C6	0.0281 (6)	0.0131 (5)	0.0212 (5)	0.0011 (4)	-0.0029(5)	-0.0006(4)	
C7	0.0264 (6)	0.0150 (5)	0.0189 (5)	-0.0017(4)	-0.0012(4)	-0.0027(4)	
C8	0.0253 (6)	0.0174 (5)	0.0155 (5)	-0.0018(4)	-0.0025(4)	-0.0019(4)	
C9	0.0234 (6)	0.0150 (5)	0.0152 (5)	-0.0007(4)	-0.0026 (4)	-0.0003 (4)	

Geometric parameters (Å, °)			
C11—C3	1.7342 (11)	C2—C3	1.4724 (16)
F1—C7	1.3545 (13)	C4—C5	1.3953 (15)
N1—H1	0.993 (16)	C4—C9	1.3957 (15)
N1—N2	1.3117 (13)	C5—H5	1.080 (16)
N1—C4	1.4055 (14)	C5—C6	1.3916 (16)
N2—C3	1.2908 (14)	C6—H6	1.071 (16)
O1—C2	1.2192 (13)	C6—C7	1.3808 (17)
C1—H1a	1.07 (2)	C7—C8	1.3837 (16)
C1—H1b	1.042 (19)	C8—H8	1.079 (16)
C1—H1c	1.05 (2)	C8—C9	1.3926 (15)
C1—C2	1.5044 (16)	С9—Н9	1.066 (17)
N2—N1—H1	121.0 (9)	C9—C4—N1	118.35 (10)
C4—N1—H1	119.6 (9)	C9—C4—C5	120.34 (10)
C4—N1—N2	119.48 (9)	H5—C5—C4	121.4 (8)
C3—N2—N1	121.70 (10)	C6—C5—C4	119.65 (11)
H1b—C1—H1a	107.7 (15)	C6—C5—H5	119.0 (8)
H1c—C1—H1a	108.0 (15)	H6—C6—C5	121.2 (9)
H1c—C1—H1b	107.7 (14)	C7—C6—C5	119.13 (11)
C2—C1—H1a	110.6 (11)	C7—C6—H6	119.7 (9)
C2—C1—H1b	109.9 (10)	C6—C7—F1	118.75 (10)
C2—C1—H1c	112.8 (11)	C8—C7—F1	119.03 (11)
C1—C2—O1	122.46 (11)	C8—C7—C6	122.22 (11)
C3—C2—O1	119.97 (10)	H8—C8—C7	120.6 (8)
C3—C2—C1	117.57 (10)	C9—C8—C7	118.67 (11)
N2—C3—C11	123.22 (9)	C9—C8—H8	120.7 (8)
C2—C3—C11	117.18 (8)	C8—C9—C4	119.98 (11)
C2—C3—N2	119.60 (10)	H9—C9—C4	119.8 (9)
C5—C4—N1	121.31 (10)	H9—C9—C8	120.2 (9)
C11—C3—N2—N1	-0.82 (12)	N1—C4—C9—C8	-179.02 (11)
C11—C3—C2—O1	3.51 (11)	N2—C3—C2—O1	-177.19 (11)
C11—C3—C2—C1	-176.28 (9)	N2—C3—C2—C1	3.02 (13)
F1—C7—C6—C5	179.68 (11)	C4—C5—C6—C7	-0.17 (14)
F1—C7—C8—C9	-179.46 (11)	C4—C9—C8—C7	-0.27 (14)
N1—N2—C3—C2	179.93 (10)	C5—C6—C7—C8	0.40 (15)
N1—C4—C5—C6	179.23 (11)	C6—C7—C8—C9	-0.18 (15)

sup-6 Acta Cryst. (2025). C81, 481-487

Hydrogen-bond geometry (Å, °)

<i>D</i> —H··· <i>A</i>	<i>D</i> —Н	$H\cdots A$	D··· A	D— H ··· A
N1—H1···O1 ⁱ	0.993 (16)	1.992 (16)	2.9196 (13)	154.5 (13)
C1—H1 <i>a</i> ···Cl1 ⁱⁱ	1.07(2)	2.83 (2)	3.7787 (13)	148.2 (15)
C1—H1 <i>b</i> ···N2 ⁱⁱⁱ	1.042 (19)	2.744 (19)	3.5452 (17)	133.7 (13)
C1—H1 <i>c</i> ···F1 ^{iv}	1.05 (2)	2.63 (2)	3.6063 (15)	153.9 (15)
C8—H8···F1 ^v	1.079 (16)	2.576 (17)	3.6171 (14)	161.8 (12)
C9—H9···O1 ⁱ	1.066 (17)	2.364 (17)	3.2335 (14)	137.8 (13)

Symmetry codes: (i) x+1, -y+1/2, z+1/2; (ii) x-1, -y+1/2, z-1/2; (iii) x-1, y, z; (iv) -x+1, -y+1, -z+1; (v) -x+2, -y+1, -z+2.

Acta Cryst. (2025). C81, 481-487